ingegneria sismica
International Journal of Earthquake Engineering
Anno XXXV – Num.4

ENHANCING THE SEISMIC PERFORMANCE OF EBFs WITH VERTICAL SHEAR LINK USING A NEW SELF-CENTERING DAMPER

Nadia M. Mirzai[1], *Reza Attarnejad*[2], *Jong Wan Hu*[3,4]

[1]School of Civil Engineering, College of Engineering, University of Tehran, P.O. Box 4563-11155, Tehran, Iran, E-mail: nmirzai@ut.ac.ir

[2]School of Civil Engineering, College of Engineering, University of Tehran, P.O. Box 4563-11155, Tehran, Iran, E-mail: attarnjd@ut.ac.ir

[3]Department of Civil and Environmental Engineering, Incheon National University, Incheon 22012, South Korea, E-mail: jongp24@inu.ac.kr

[4]Incheon Disaster Prevention Research Center, Incheon National University, Incheon 22012, South Korea

SUMMARY: *Conventional seismic resisting structural systems may be subjected to permanent deformation and damage through strong earthquakes, which can induce considerable post-earthquake repair costs. This paper presents an easy and fast way to reduce link plastic rotation demand, residual link plastic rotation, maximum absolute floor acceleration repair costs, time and also a system for seismic retrofitting of the eccentrically braced frames (EBFs): a self-centering inverted Y-braced EBF system that combines shape memory alloy bars and lead rubber damper (SMA-LRD). Four and nine-story steel frames are designed and analyzed with and without the proposed system to quantify their seismic performance using the OpenSees. Over 5000 nonlinear time history analyses were conducted to evaluate the seismic performance of proposed hybrid device using 28 ground motion records. The results of incremental dynamic analyses (IDA) show that implementing the new system leads to a considerable reduction in maximum drifts, residual drifts, and residual displacements.*

KEYWORDS: *Self-centering, SMA, LRD, EBF, Residual drift, OpenSees, IDA*

1 Introduction

Even if a building does not collapse, it may not be possible to repair it or, in a better scenario, the process of restoration would be both cost- and time-consuming. Thus, the design of structures considering rapid repair scenarios (e.g. localized damage in the places that are easy to inspect and easy and economical to repair) or buildings that are inelastic but have limited structural or nonstructural damage (i.e. isolated structures, stiff systems with small lateral displacements to limit structural and nonstructural damage, and can be reoccupied quickly) would seem to be the direction to go for the modern society [Deierlein, 2009, Roh *et al.*, 2018]. The primary notion in the design of eccentrically braced frames (EBFs) is combining the advantages of both concentrically braced frames (CBFs) and moment resisting frames (MRFs) into a single structural system [Kazemzadeh Azad and Topkaya, 2017, Montuori *et al.*, 2016a, 2016b, 2017]. There are various shapes for an EBF system. Compared to their

Corresponding author: Jong Wan Hu, Department of Civil Engineering, Incheon National University, Incheon 22012, South Korea, E-mail: jongp24@inu.ac.kr

horizontal counterparts, inverted Y- braced EBFs (also known as EBFs with vertical links) have a simpler post-earthquake repair procedure [Bosco *et al.*, 2016, Montuori *et al.*, 2016a, Nastri, 2016]. Moreover, inverted Y-braced EBFs can be easily employed for the seismic retrofitting of existing buildings. The key distinguishing feature of an EBF system is that the link is designed to enable energy dissipation and ductility through yielding subjected to design basis earthquakes [Mansouri *et al.*, 2012], while all other structural elements are designed to be stronger than the link and behave elastically [Montuori *et al.*, 2014a, 2015, Xu *et al.*, 2016]. In fact, the link dissipates seismic energy via plastic deformation and acts as a passive energy dissipative device. Almost the same idea has been employed in the added damping and stiffness (ADAS) device, yielding shear panel device, metal damper, and so on [Chan and Albermani, 2008, Chan *et al.*, 2009, Farzampour and Eatherton, 2018a, 2018b] and also using friction damper in the place of link members [Montuori *et al.*, 2014b]. However, after a strong earthquake, the plastic deformation of links can lead to permanently deformed frames whose repair is difficult.

Several previous studies have indicated that residual drift, which arises from nonlinear behavior of yielding elements of a structural system, can play a significant role in determining the performance of a structure after the earthquake and for assessment of potential damage [Silwal *et al.*, 2016]. Residual displacement has a considerable effect in judging the post-earthquake safety of buildings, as well as in the decision on the economic possibility of repair and reconstruction [Erochko *et al.*, 2011].

To address this issue, two different scenarios are available. The first is using a replaceable link beams by employing bolted endplate connections instead of welded connections [Xu *et al.*, 2016]. The possibility of applying replaceable links to EBFs was clearly shown by [Dubina *et al.*, 2008]. The second scenario is applying a new class of seismic resisting systems with excellent self-centering ability. Several remarkable efforts have been made to extend self-centering seismic resisting systems to minimize the residual deformation issue. For example, Ricles et al. developed the post-tensioned steel strands anchored at the column flange and parallel to the beams [Ricles *et al.*, 2002]. With improving the technology, the concept of employing energy dissipater equipment has been developed to control the response of structures in dynamic loads [Mansouri *et al.*, 2017, Zeynali *et al.*, 2018]. In this paper, the hybrid passive control system includes a device like a lead-rubber bearing (LRB).

The objective of this paper is to evaluate the seismic performance of the SMA-LRD system under earthquake events. Four- and nine-story steel frames are analyzed, using OpenSees, with and without the proposed system to quantify their collapse performance.

2 Shape memory alloy description

2.1 Mechanical properties

Shape memory alloy (SMA) is a new smart material with the recentering capability. This material manifests two important behaviors that makes it as a special material because of the changes in either stress or temperature. One is the shape memory effect, which causes SMAs return to the initial shape by cooling after heating to transfer from the martensite to austenite phase, and the other is the superelastic effect (SE), that can recover its initial condition when the stresses omit and can come back to the original shape with a very small residual strain. These two effects are related to its crystal phases [Seo *et al.*, 2015]. As shown in Figure 1, the

SE phase happens at lower stresses and a higher temperature than the austenite finishing temperature ($T>A^f$), while the shape memory effect occurs at higher stresses and a lower temperature than the martensite finishing temperature ($T<M^f$) [Gao *et al.*, 2016].
One of the most well-known SMA materials is nickel-titanium (NiTi) with a special ability to maintain large strains (e.g. 6-8%) that are crystallographically reversible, thereby sustaining the material without residual deformation [DesRoches *et al.*, 2004, Hu, 2008]. The used NiTi bars adopted from [DesRoches *et al.*, 2004] have a very low austenite start temperature and the composition is based on the average of 56.0% nickel by weight and 44.0% titanium. Table 1 presents the full properties of the used NiTi. Also, based on [DesRoches *et al.*, 2004], the residual strain of NiTi after applying 6% cycle strain is less than 0.75%. The defined parameters in Table 1 can be seen in Figure 1.

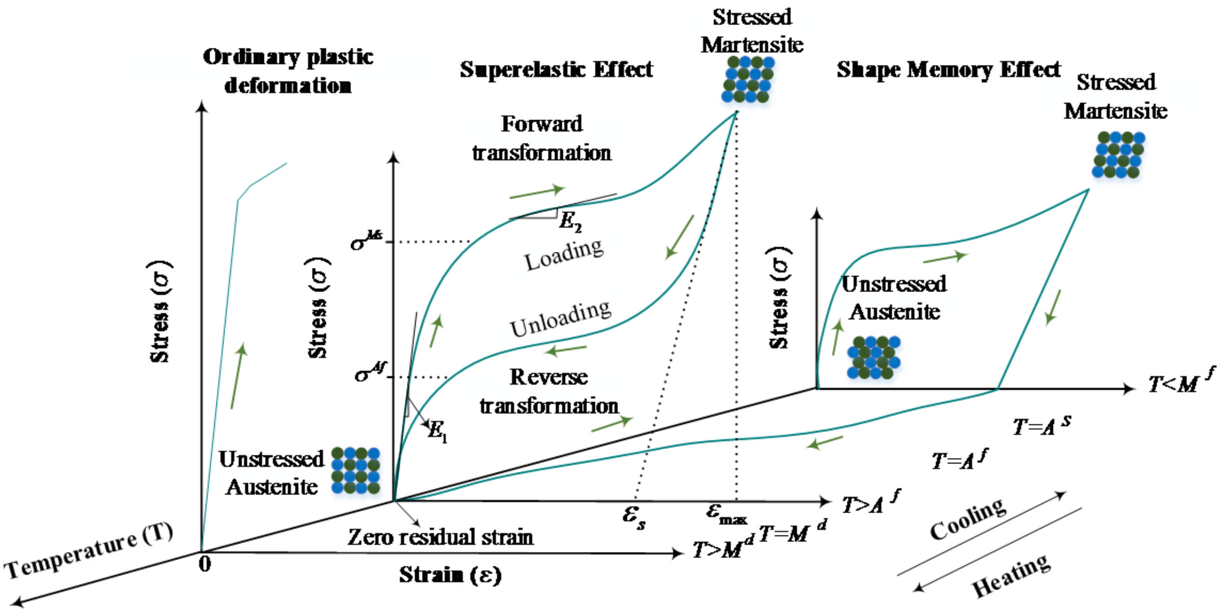

Figure 1 - *Stress-strain-temperature relationships in SMA* [Seo *et al.*, 2015]

Table 1 - *Full properties of used NiTi* [DesRoches *et al.*, 2004]

Properties	NiTi SMA
Physical properties	
Density	6.45 g/cm^3
Mechanical properties	
Recoverable elongation, ε_{max}	up to 8%
Modulus of elasticity E_1	24000 MPa
Modulus of elasticity E_2	0.308 E_1
Austenite to martensite starting stress, σ^{Ms}	270 MPa
Martensite to austenite finishing stress, σ^{Af}	70 MPa
Poisson's ratio	0.33
Chemical properties	
Corrosion performance	Excellent (similar to stainless steel)

2.2 Previous research on the SMA application

In recent years, due to its self-centering ability in addition to energy dissipation aspects, SMA has become an object of considerable research attention. Specifically, many studies focused on the seismic performance of structures equipped with SMA. For instance, [Hu and Leon, 2011] proposed a new type of bolted joints which combines the low carbon steel and SMA components. In addition, [Seo *et al.*, 2015] suggested steel slit dampers equipped with SMA which can dissipate considerable energy during cyclic loading. Many researchers [Rofooei and Yadegari Farzaneh, 2016] investigated the effect of SMA bolts in improving the seismic behavior of joints in steel MRFs. Their results show that using SMA bolts can reduce the seismic response. Moradi and Alam [Moradi and Alam, 2015] presented a new beam to column connection equipped with shape memory alloy to mitigate the residual drift and display an effective ductility. Several studies also showed the efficiency of lead rubber dampers in reducing the seismic response of structures [Hu, 2016, Leblouba *et al.*, 2015, Mansouri *et al.*, 2017]. Some other researchers demonstrated that the combination of base isolation and SMA leads to more structural integrity and concluded that recentering LRB isolators cause an improvement of seismic performance in terms of energy dissipation and recentering influence [Hu, 2016]. Recently, [Hedayati Dezfuli and Alam, 2017] presented a smart elastomeric isolator equipped with ferrous SMA wires. Furthermore, [Zareie *et al.*, 2017a, 2017b] proposed a novel SMA-braced frame which works in both compression and tension. [Billah and Shahria Alam, 2016] developed the SMA bridge piers based on the performance-based design concept and demonstrated the efficiency of SMA for reduction of residual drift of concrete elements.

3 Proposed passive system

Since the LRD has a shear mechanism, an inverted Y-Shaped braced frame is considered to evaluate the behavior of the SMA-LRD device. The inverted Y-Shaped braced frame is one type of the EBFs which includes a vertical link as a shear fuse so that the existing shear forces of the floor are transferred from the rigid diaphragm to the shear link during an earthquake. This vertical link dissipates energy and provides ductility by shear yielding in the link's web [Bouwkamp *et al.*, 2016]. Even though this system covers some disadvantages of EBFs, but yielding the steel link to dissipate energy causes a large deformation and residual drift [Bouwkamp *et al.*, 2016].

In the new SMA-LRD braced frame, the LRD is replaced with the steel link beam, while the employed SMA bars play the role of recentering behavior (see Figure 2).

This self-centering behavior leads to a reduction of residual drifts and makes a uniform drift. In this system, the floor shear force transfers to the SMA-LRD device and the other parts of the structure remain elastic. Therefore, LRD dissipates energy and the SMA bars not only dissipate energy, but also recenter the structure and decrease the residual drift, residual displacement, and make a more uniform displacement.

The connection of SMA bolts and steel plates is made using the nut .The SMA bars can slip inside of the plates. It means that when the applied force moves the upper plate to right, the green plates work and the yellow bars are in the tension associated with the energy dissipation but when the force is inversed, the upper plate moves to left, hence the yellow plates and the pink bars play the role of the damper and recenter the deformations. Figure 3 shows the deformed shape of the SMA-LRD.

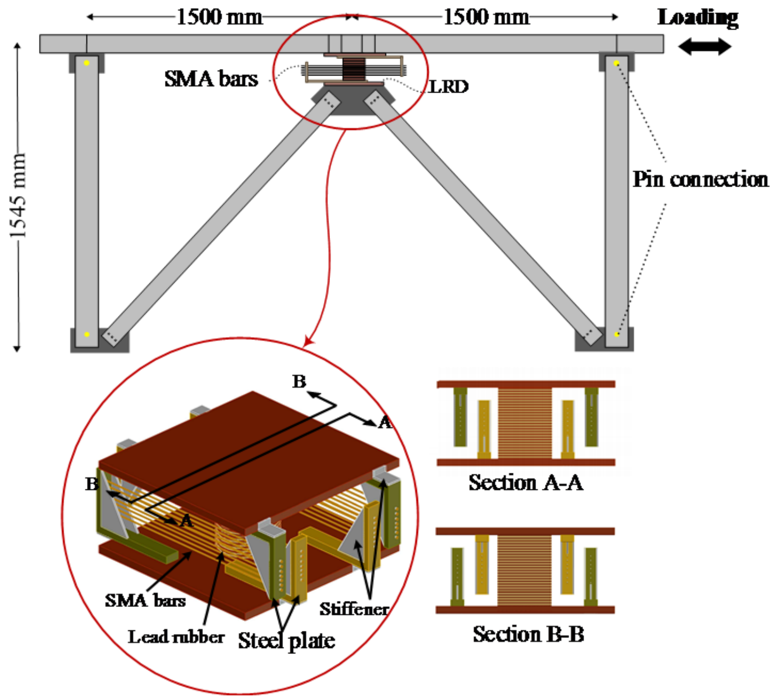

Figure 2 - *Proposed SMA-LRD device*

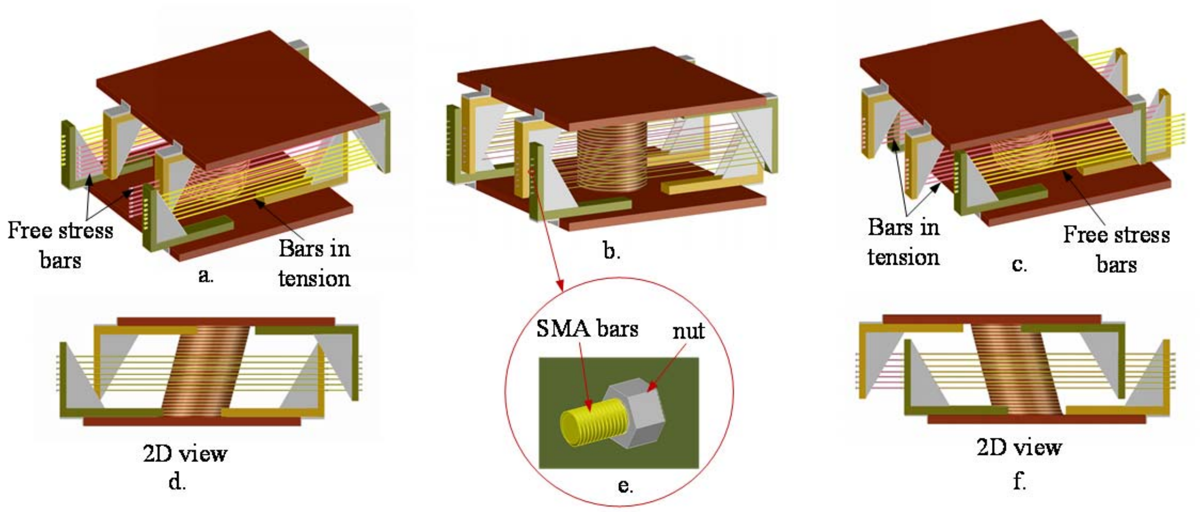

*The pink and yellow bars are both SMA (NiTi). The different color is just for recognizing

Figure 3 - *a. Deformed shape of LRD, b. 3D view of LRD, c. deformed shape of LRD, d. 2D view of the deformed shape of LRD, e. connection of SMA and steel plates, f. 2D view of the deformed shape of LRD*

4 Analytical modeling

4.1 Verification study

Since verification study is essential for each numerical study, a single-story inverted Y-Shaped braced frame is adopted from the experimental test [Bouwkamp *et al.*, 2016] (see Figure 4). To verify the modeling, specimen number three of the mentioned research was considered (see Table 2 and Table 3). The SDOF building was subjected to a cyclic loading: two-cycle is applied at the displacement levels of ± 1.5 mm, ± 2.0, ± 3.0, ± 3.5, ± 4.0, ± 5.0, ± 6.0, ... , ± 10.0, ± 12.0, ..., ± 34.0. Figure 5 shows the applied loading protocol. The specimen 3 has been designed to have shear yielding but the other specimens have been designed to behave in both shear and flexure.

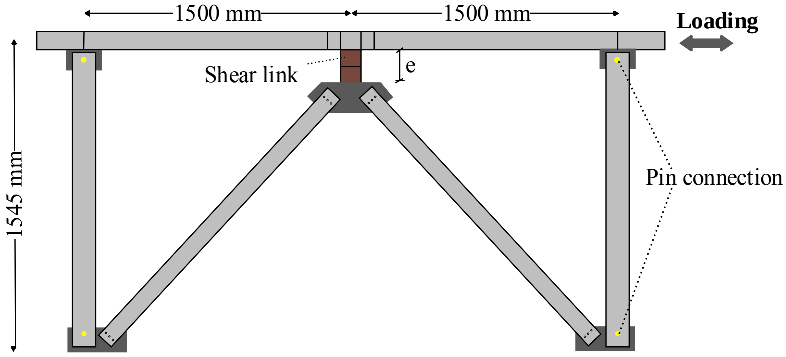

Figure 4 - *Geometry of verified model*

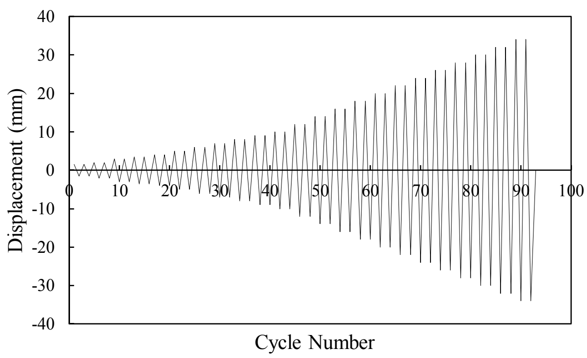

Figure 5 - *Loading protocol* [Bouwkamp *et al.*, 2016]

Table 2 - *The details of the tested specimens* [Bouwkamp *et al.*, 2016]

Specimen No.	Beam section	Vertical shear link section	Shear link length, *e* (mm)	Column section	Brace section
3	HEA320	HEA280	300	2UPN140	2UPN220

Table 3 - *Strength results of shear link* [Bouwkamp *et al.*, 2016]

	Theoretical values		Testing results			
Specimen No.	V_p (kN)	M_p (kN.m)	V_y (kN)	V_u (kN)	g_u(Rad)	M_{bot}/M_{top}
3	299	333.6	290	600	0.113	0.81

In Table 3, V_p,M_p, V_y, g_u, and M_{bot}/M_{top} are referred to the nominal shear strength of the link, nominal plastic flexural strength, yielding shear, ultimate shear, rotation of the shear link, and the ratio of the end moment link, respectively. The response of the one story building was obtained under experimental cyclic loading. The results are compared in Figure 6 which is showing well agreement with the experimental test.

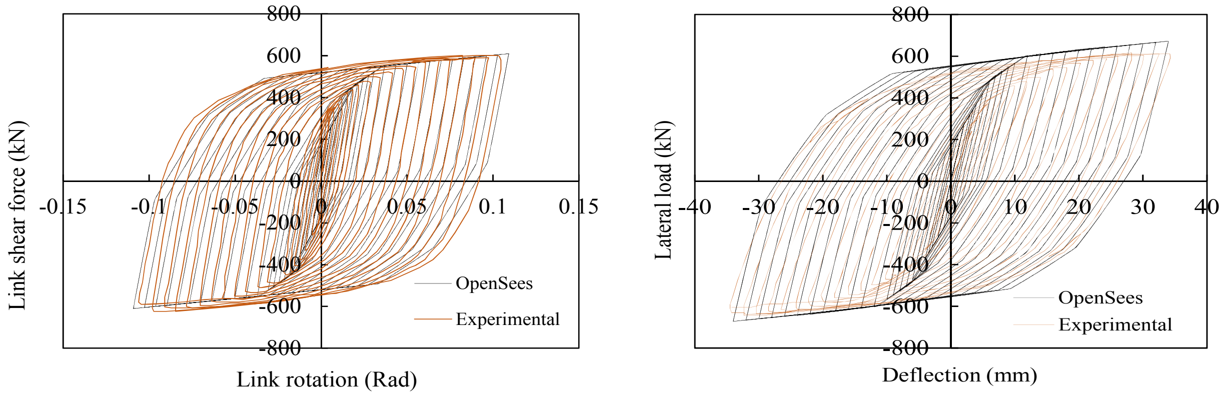

Figure 6 - *Comparison between OpenSees and experimental results conducted by* [Bouwkamp et al., 2016]

4.2 Detailed modeling in OpenSees

In this study, the investigation of the seismic behavior of 4- and 9-story buildings was performed in the OpenSees platform [OpenSees]. This software is one of the powerful finite element programs to evaluate the global behavior of the structures. The second order effect includes both 1) large deflections and 2) material nonlinearity. The large deformation is considered by adding the leaning column to apply the effect of the gravity columns the model. The gravity columns cause to consider the effect of the additional moments of the columns. The material nonlinearity also is taken into account by using the *Steel02* and *nonlinearBeamColumn element* in OpenSees. All beams, columns, and braces are simulated by *nonlinearBeamColumn* with a fiber section. The *Giuffre-Menegotto-Pinto* model *(Steel02)* with isotropic strain hardening 0.025 is considered for all mentioned elements. This kind of element and material property are taken into account the material nonlinearity. All beams and braces are end-pinned elements by two springs *(zeroLength* element) with high stiffness in two translational directions. The rigid diaphragm is considered using the *equalDOF* command in each floor. In addition, according to [Popov and Ricles, 1994] nonproportional viscous damping was used by *Region* command and no viscous damping was applied to the vertical link. Furthermore, an imperfection of $L/1000$ *(L* is the length of braces) is assigned to the braces to consider the buckling. In addition, the P-Δ effect is considered using leaning column. Actually, the leaning column is used to consider the effect of the additional moments which are applied to the lateral-force-resisting columns by gravity columns. Two important part of the modeling are steel vertical link and SMA-LRD damper.
Steel vertical link is simulated according to the Popov's improved model.
For modeling of the SMA-LRD, the behavior of the damper is simulated by two parallel springs (Figure 7).

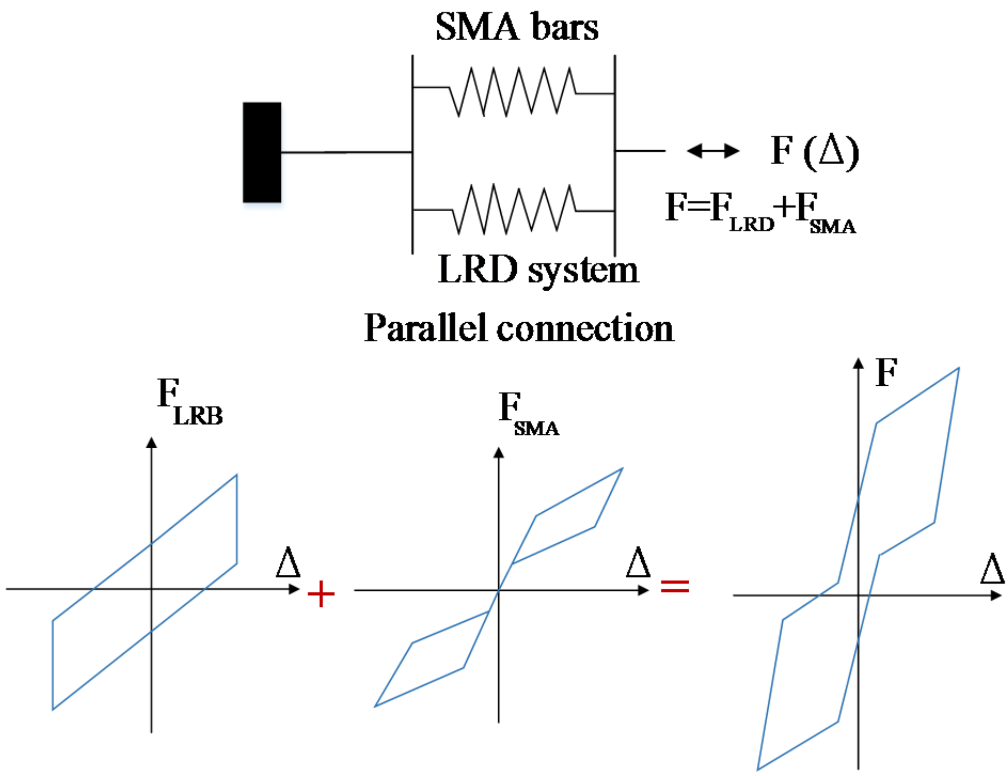

Figure 7 - *SMA-LRD modeling*

To simulate the SMA bars, *SelfCentering* material (flag shaped) is adopted from the library of the OpenSees platform which can consider the residual strain effect. The details of the material behavior are shown in Figure 8.

In Figure 8 the k_1 and k_2 are the initial stiffness and post-activation stiffness ($0< k_2< k_1$), respectively. *SigAct* refer to forward activation stress/force and *epsSlip* is the slip strain/deformation (there will be no slippage if espSlip=0), *epsBear* is the bearing strain/deformation (there will be no bearing if the epsBear=0) and the *rBear* is the ratio of the bearing stiffness to initial stiffness (k_1).

To verify the behavior of the SMA, the experimental test which has been conducted by DesRoches et al. [DesRoches *et al.*, 2004] was used. The properties of the used SMA material are listed in Table 1. Figure 9 shows the results of a comparison between experimental results and the OpenSees modeling which demonstrates a good agreement. To simulate the LRB, *Steel01* material is used [OpenSees]. The study of [Avossa and Pianese, 2017] demonstrates that high damping LRB causes a reduction of the devices displacements and to advantageous or lower damaging effects on the superstructure.Table 4 presents the property of the used LRB. In Table 4, V is the vertical load, K_e is effective horizontal stiffness, x_e is equivalent viscous damping coefficient, d_1, F_1, d_2, F_2 define the bilinear curve, D_g is external elastomer diameter, t_e is total elastomer thickness, h is height excluding outer steel plates, H is total height including outer steel plates, and Z is side length of outer steel plate. Figure 10 illustrates that the OpenSees results trend the expected treat of the LRB. Figure 11 shows the behavior of the one-story building equipped with SMA-LRD force-displacement diagram.

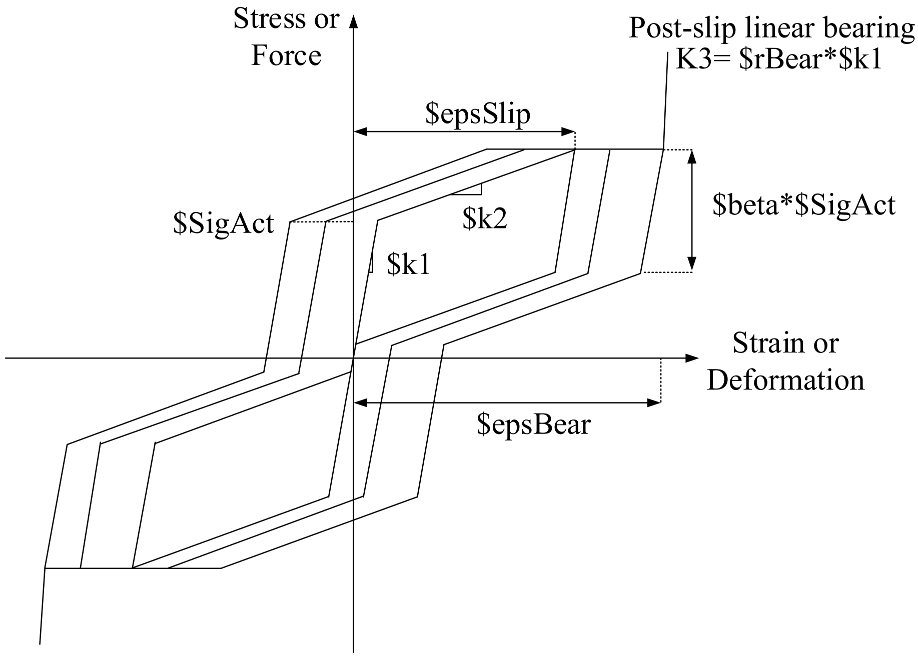

Figure 8 - *SelfCentering material* [OpenSees]

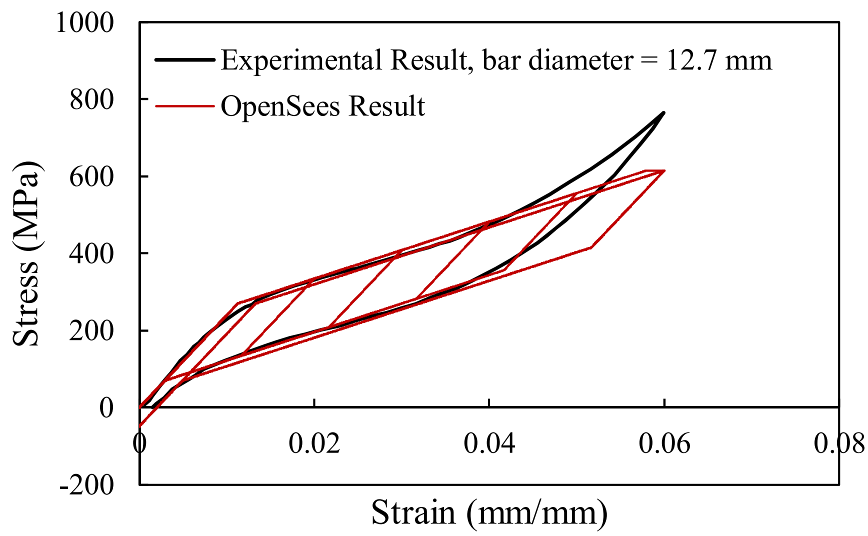

Figure 9 - *Comparison between OpenSees and experimental results conducted by* [DesRoches *et al.*, 2004] *for SMA bars*

Table 4 - *The properties of LRB* ["FIP Industriale Company, Italy,"]

LRB model	V (kN)	K_e (kN/mm)	ξ_e (%)	F_2 (kN)	F_1 (kN)	d_1 (mm)	D_g (mm)	t_e (mm)	h (mm)	H (mm)	Z (mm)
S 500/100-110	2700	1.94	35	162	106	8	500	100	197	247	550

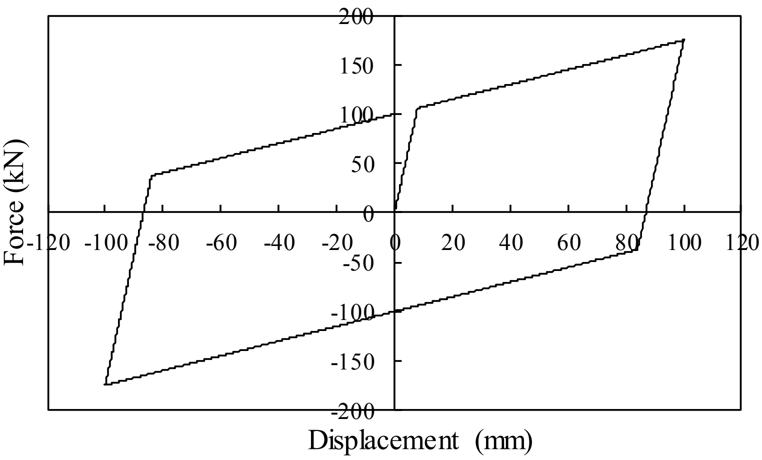

Figure 10 - *The force-displacement of LRD and SMA by OpenSees*

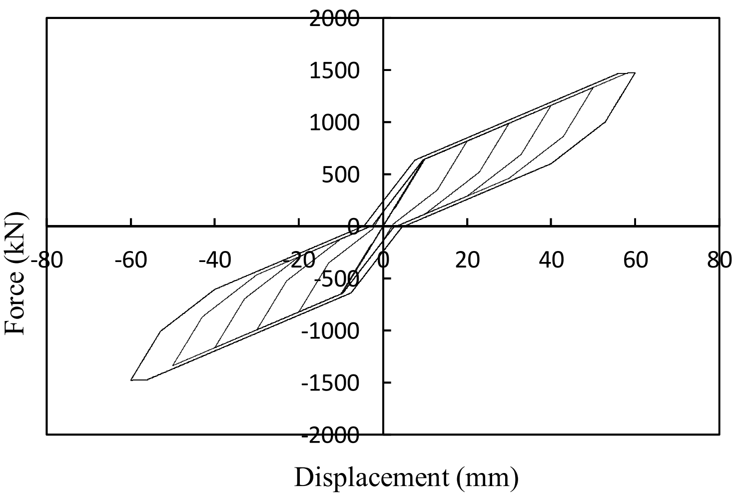

Figure 11 - *SMA-LRD force-displacement diagram by OpenSees*

4.3 Design of structures

To investigate the seismic performance of the SMA-LRD device, four- and nine-story 3D inverted Y-shaped braced frames are studied. These frames are designed based on AISC 2010 LRFD provisions. The shear links are designed for shear yielding. Figure 12 shows the plan and views of structures. The dead and live loads are 5.4 kN/m^2 and 2 kN/m^2 for the roof story and 5.0 kN/m^2 and 2.0 kN/m^2 for other stories, which are applied to the story level as the distributed loads. The leaning column carrying gravity loads are connected to the frame to simulate P-Δ effects. The selected member sections for the four- and nine-story frames are listed in Table 5.

For a better understanding about the effect of the SMA-LRD, the SMA-LRD braced frames are not designed again and just the shear link (vertical link) is replaced with the device. Therefore, the beams, columns, and braces are the same as in the IY-Shaped braced frame. The properties of the SMA bars and LRD are listed in Table 6.

Table 5 - *The member sections of four- and nine-story IY-Shaped brace frames*

		Section (European standard profiles)						Link length (mm)
		Beam		Column				
Frame	Story No.	B1 (Figure 12)	B2 (Figure 12)	C1 (Figure 12)	C2 (Figure 12)	Brace	Link	
4-Story	1	IPE240	IPE330	Box 100×100×10	Box 180×180×20	2UPN200	IPE450	350
	2	IPE240	IPE330	Box 100×100×10	Box 140×140×20	2UPN200	IPE450	350
	3	IPE240	IPE330	Box 80×80×10	Box 120×120×10	2UPN180	IPE400	350
	4	IPE240	IPE270	Box 70×70×10	Box 70×70×10	2UPN160	IPE300	350
9-Story	1	IPE330	IPE400	Box 160×160×10	Box 400×400×25	2UPN220	IPE400	480
	2	IPE330	IPE400	Box 160×160×10	Box 400×400×25	2UPN220	IPE550	480
	3	IPE330	IPE400	Box 140×140×10	Box 400×400×25	2UPN220	IPE600	480
	4	IPE330	IPE400	Box 120×120×10	Box 400×400×25	2UPN220	IPE600	480
	5	IPE330	IPE400	Box 120×120×10	Box 400×400×25	2UPN220	IPE600	350
	6	IPE330	IPE400	Box 100×100×10	Box 400×400×25	2UPN220	IPE450	350
	7	IPE330	IPE400	Box 100×100×10	Box 400×400×25	2UPN220	IPE600	350
	8	IPE330	IPE400	Box 70×70×10	Box 400×400×25	2UPN220	IPE600	350
	9	IPE330	IPE270	BOX70x70x10	BOX70x70x10	2UPN180	IPE600	350

Table 6 - *The properties of the SMA-LRD devices in 4- and 9-story buildings*

Frame	SMA braced frame			
	Story No.	Total area of SMA bars (mm^2)	SMA length (mm)	LRD properties
4-story	1	1900	850	Table 4
	2	1700	500	Table 4
	3	800	350	Table 4
	4	500	350	Table 4
9-story	1	2100	800	Table 4
	2	1900	800	Table 4
	3	1900	800	Table 4
	4	2000	800	Table 4
	5	1600	800	Table 4
	6	1100	800	Table 4
	7	900	800	Table 4
	8	700	800	Table 4
	9	600	800	Table 4

To select the dimension of the LRD, the product of the FIP LRB company ["FIP Industriale Company, Italy,"] is used. The type of the LRD is determined according to the height and width of the device. Also, the vertical load and the maximum displacement of the device based on the structure interstory drift are the important parameters to choose the type of the device.

5 Incremental dynamic analysis

Incremental dynamic analysis (IDA) is used to assess and compare the plastic mechanisms of the steel EBFs with and without proposed dampers. In fact, IDA curves help to find out the natural random variability within the ground motion records which need a statistical assessment [De Matteis *et al.*, 2018]. For the IDA, 5% damped spectral acceleration at the fundamental period of the structure, S_a (T_1,5%), as the intensity measure (IM) is repeatedly increased until global instability or collapse occurs [Alfano, 2017, Vamvatsikos and Cornell, 2002].

The maximum interstory drift ratio, maximum residual drift ratio and maximum absolute floor acceleration are adopted as damage measure (DM) parameters. In this paper, interstory drift ratio and the link plastic rotation are adopted as DMs. Here, the link plastic rotation, γ_p, is given as the difference of link ends displacements divided by link length [Nastri *et al.*, 2015]. Engineering design is based on the mean, median, or 84% of a DM. Hence, the 16%, median, and 84% curves for the considered ground motion records are considered as statistical assessment which is more reliable and convenient to use [Hedayati Dezfuli and Alam, 2015, Petrone *et al.*, 2017].

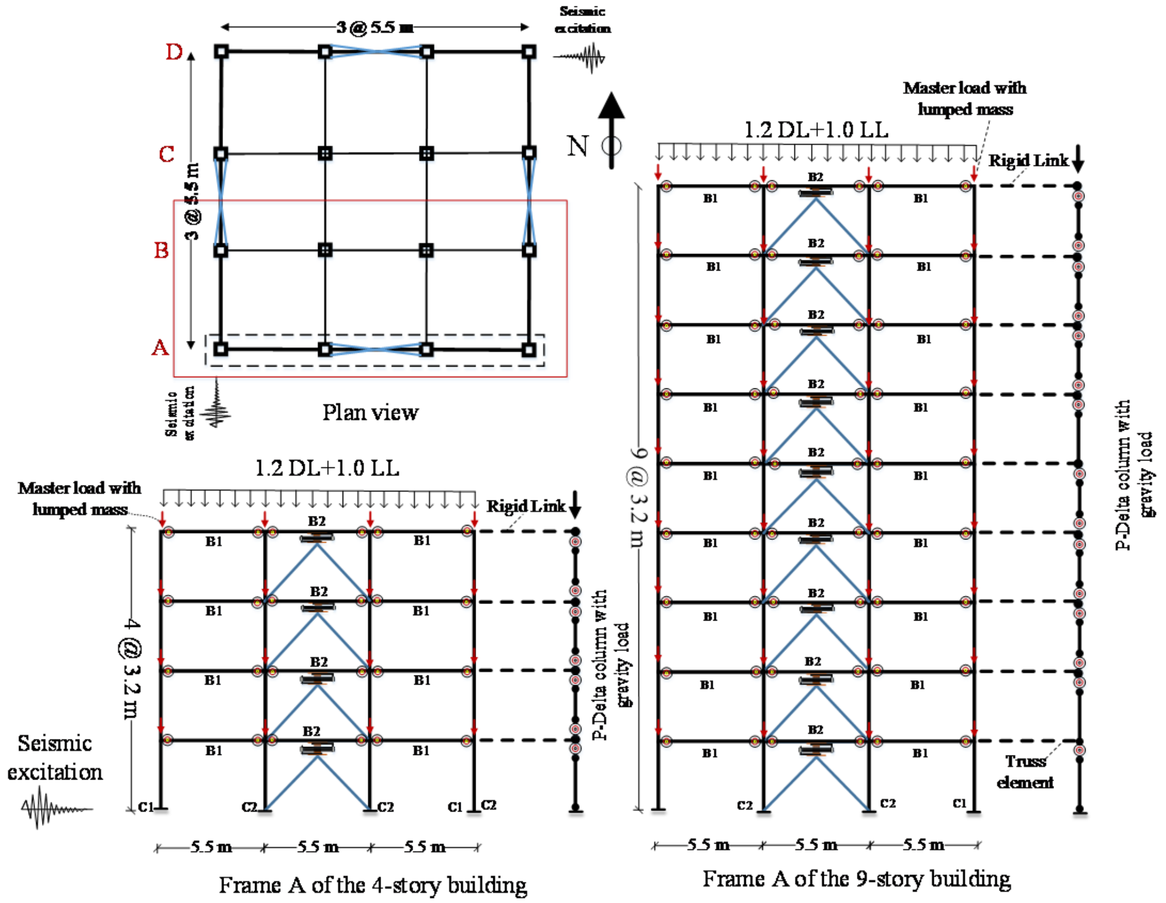

Figure 12 - *Structural configuration of four and nine-story buildings considering leaning columns*

In this study, 28 far-field ground motions are selected from [FEMAP695, 2009] which are available on the PEER NGA database to do IDA analyses on each archetype according to the FEMA P695 methodology [FEMAP695, 2009]. The numerical model of the buildings is developed in 2D and two cases is evaluated: with and without the SMA-LRD. 5040 nonlinear time history analyses were performed using OpenSees platform. After post-processing the data in the MATLAB environment, the IDA response plots are created.

5.2 Maximum link plastic rotation

The maximum link plastic rotation (MLPR) is an important index of EBF behavior in performance-based seismic analysis; this section presents the variation in MLPR during the IDA. Figure 13 shows maximum link plastic rotation IDA curves for conventional and SMA-LRD frames, where a data point in each curve specifies the MLPR of the structure subjected to an earthquake scaled at a specific spectral acceleration. The plot provides the indications for each of 28 records. The dashed lines show the boundaries of life safety (LS) and collapse prevention (CP) performance levels according to [ASCE41-17, 2017]. The plastic rotation angle of the link beam for the LS and CP limit states are 0.14 and 0.16 radian, respectively [ASCE41-17, 2017]. It is clear that the SMA-LRD frame could improve the seismic performance of conventional EBF.

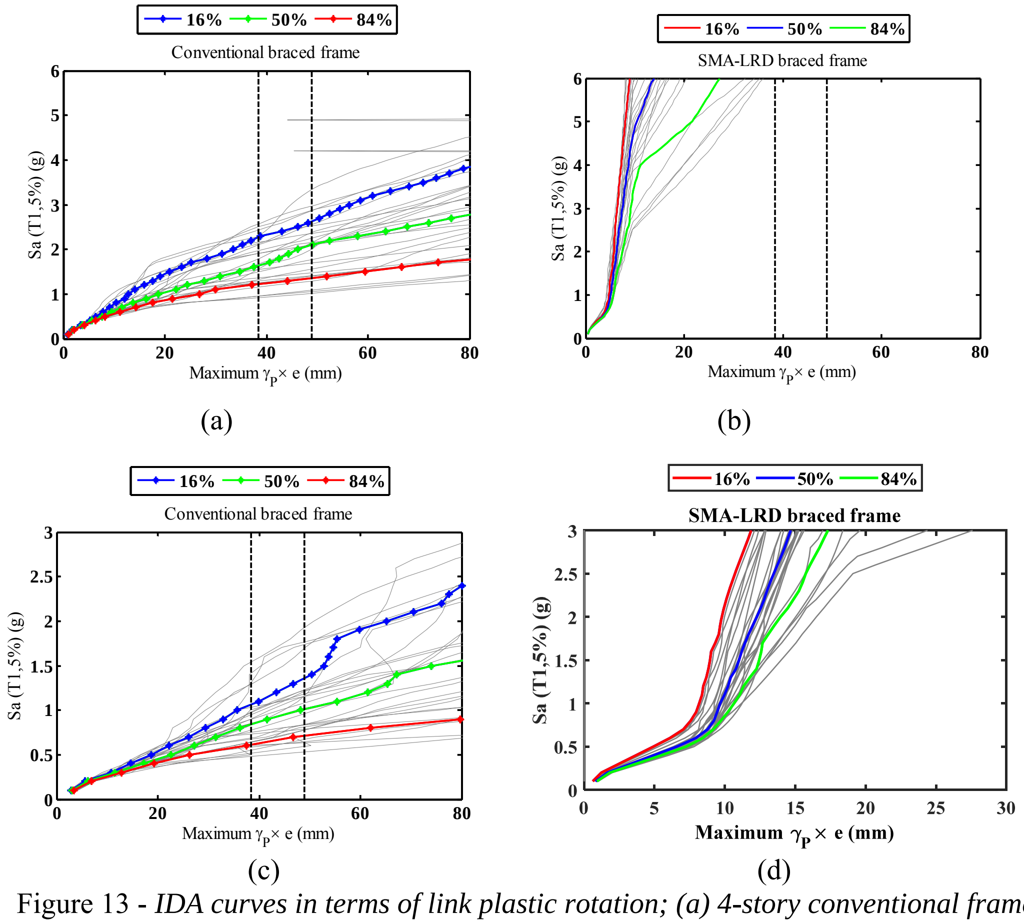

Figure 13 - *IDA curves in terms of link plastic rotation; (a) 4-story conventional frame (b) 4-story SMA-LRD frame (c) 9-story conventional frame (d) 9-story SMA-LRD frame*

5.3 Maximum residual link plastic rotation

Supplying the structure with a recentering ability, defined as the capability of minimizing the residual deformations after the end of the earthquake. To find the residual values, extra zero values are added to the end of the ground of the motion (in this study 25 seconds), the structure vibrate freely after the ground motion, then the residual value (e.g. drift) is the last value in the recorder file.

Figure 14 shows the maximum residual link plastic rotation IDA curves for 4- and 9-story structures. The results denote a considerable reduction in the residual deformation at various levels of ground motions when the SMA-LRD is employed as the control device which can highly reduce the repair cost of post-earthquake conditions.

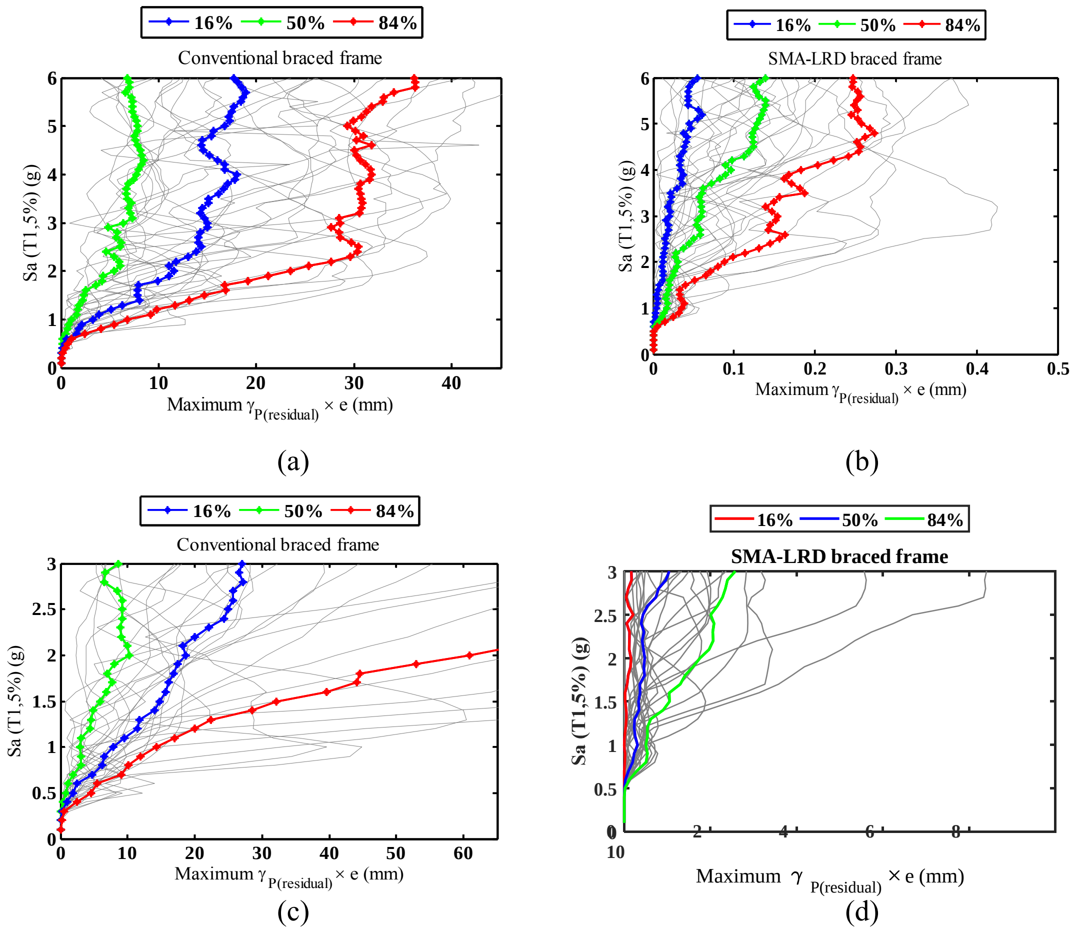

Figure 14 - *IDA curves in terms of residual link plastic rotation; (a) 4-story conventional frame (b) 4-story SMA-LRD frame (c) 9-story conventional frame (d) 9-story SMA-LRD frame*

5.4 Maximum absolute floor acceleration

Maximum floor acceleration is related to damage in non-structural components [Silwal *et al.*, 2016]. Figure 15 shows the profiles of maximum absolute floor acceleration at the maximum considered earthquake (MCE) level. MCE is defined as 1.5 time of the design basic earthquake (DBE) [ASCE7-10, 2010].

Results revealed that, for all the ground motions, the maximum floor acceleration in the structures equipped with SMA-LRD device tends to reduce which can reduce the cost of repairs after the earthquake.

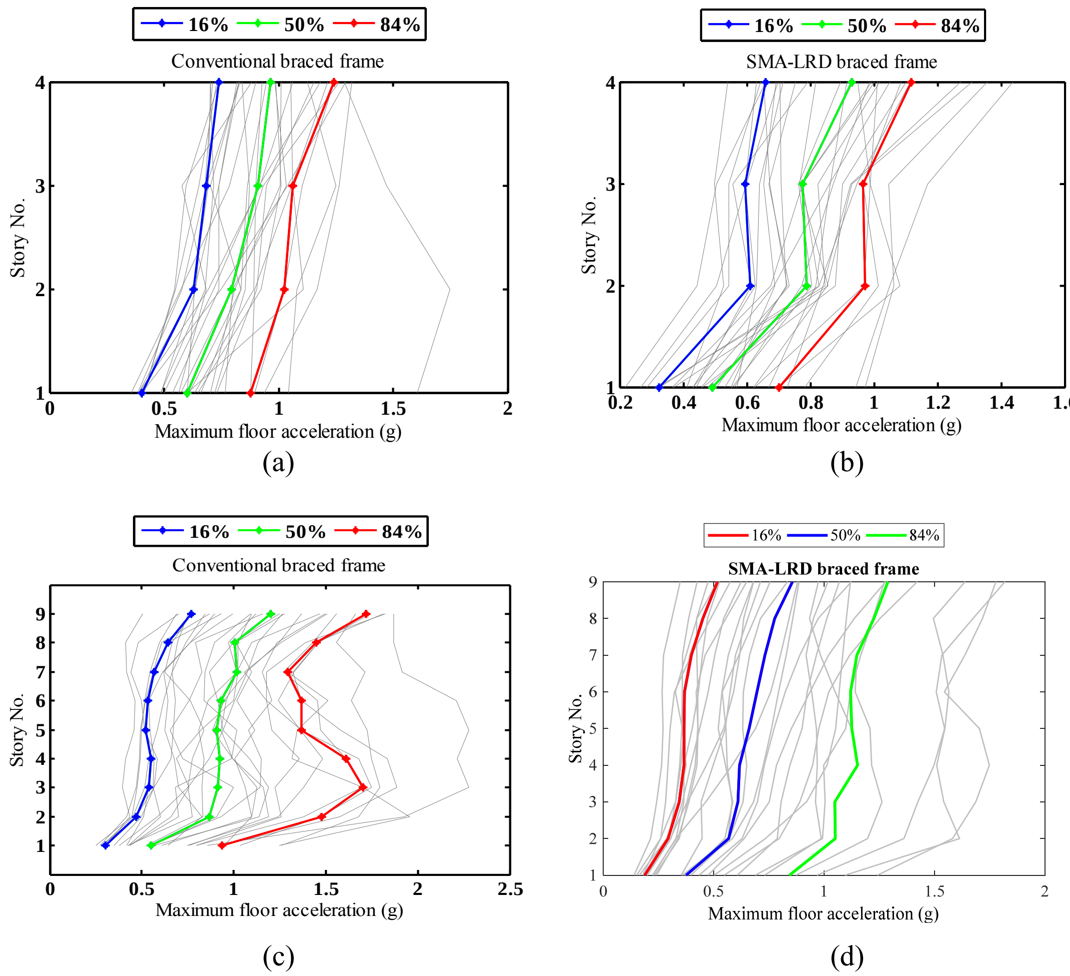

Figure 15 - *Maximum absolute floor acceleration at MCE level; (a) 4-story conventional frame (b) 4-story SMA-LRD frame (c) 9-story conventional frame (d) 9-story SMA-LRD frame*

6 Conclusions

In this paper, a recentering seismic-resistant system (denoted as SMA-LRD) including an eccentrically braced frame equipped with shape memory alloy which is a rapid repair fuse was proposed and numerically evaluated. The modeling techniques of link beam, LRD, and SMA were validated using the experimental results available in the literature. Four- and nine-story steel frames were considered as case numerical models. Nonlinear time history analysis was conducted using ten different ground motions simulated in the OpenSees platform. The main findings of the present study are as follows:

1. Simulation results illustrate that the SMA-LRD is capable of mitigating maximum link plastic rotation in both 4- and 9-story buildings.
2. As compared to conventional EBFs, the SMA-LRD system effectively reduces the residual link plastic rotation for the studied buildings at different ground motion

records.
3. Maximum floor acceleration for the SMA-LRD system was lower than conventional EBF system which leads lower damage in non-structural components.
4. Considerably lower residual deformations that were observed in the proposed SMA-LRD system demonstrate that the repair costs of the steel buildings equipped with SMA-LRD are lower than those of the traditional steel frames after an earthquake.
5. The efficiency of the proposed system improves with increasing the number of stories. A comparison between the results of 4- and 9-story buildings indicates that the percentage decrease for the 9-story building is higher in terms of maximum interstory drift, residual drift, and residual displacement.

7 Acknowledgements

This research was supported by a grant (18SCIP-B146946-01) from Construction technology research program funded by the Ministry of Land, Infrastructure and Transport of Korean government.

References

Alfano, G. (2017). Seismic reliability assessment of yielding baseisolated structures for an intermediate isolation degree. Ingegneria Sismica, **34**(3-4), 25-37.

ASCE7-10 (2010), "ASCE 7-10, ASCE/SEI: Minimum design loads for buildings and other structures: American Society of Civil Engineers", USA.

ASCE41-17 (2017), "ASCE standard, ASCE/SEI 41-17, seismic evaluation and retrofit of existing buildings", Reston, USA.

Avossa, A.M. and Pianese, G. (2017). Damping effects on the seismic response of base-isolated structures with LRB devices. Ingegneria Sismica, **34**(2), 3-29.

Billah, A.H.M.M. and Shahria Alam, M. (2016). Plastic hinge length of shape memory alloy (SMA) reinforced concrete bridge pier. Engineering Structures, **117**(15), 321-331.

Bosco, M., Ghersi, A., Marino, E.M. and Rossi, P.P. (2016). Importance of link models in the assessment of the seismic response of multi-storey ebfs designed by ec8. Ingegneria Sismica, **33**(3), 82-93.

Bouwkamp, J., Vetr, M.G. and Ghamari, A. (2016). An analytical model for inelastic cyclic response of eccentrically braced frame with vertical shear link (V-EBF). Case Studies in Structural Engineering, **6**, 31-44.

Chan, R.W.K. and Albermani, F. (2008). Experimental study of steel slit damper for passive energy dissipation. Engineering Structures, **30**(4), 1058-1066.

Chan, R.W.K., Albermani, F. and Williams, M.S. (2009). Evaluation of yielding shear panel device for passive energy dissipation. Journal of Constructional Steel Research, **65**(2), 260-268.

De Matteis, G., Brando, G., Caldoso, F. and D'Agostino, F. (2018). Seismic performance of dual steel frames with dissipative metal shear panels. Ingegneria Sismica, **35**(2), 124-141.

Deierlein, G.G. (2009), "Report of the First Joint Planning Meeting for the Second Phase of NEES/E-Defense Collaborative Research on Earthquake Engineering".

DesRoches, R., McCormick, J. and Delemont, M. (2004). Cyclic properties of superelastic shape memory alloy wires and bars. Journal of Structural Engineering, **130**(1), 38-46.

Dubina, D., Stratan, A. and Dinu, F. (2008). Dual high-strength steel eccentrically braced frames with removable links. Earthquake Engineering and Structural Dynamics, **37**(15), 1703-1720.

Erochko, J., Christopoulos, C., Tremblay, R. and Choi, H. (2011). Residual drift response of SMRFs and BRB frames in steel buildings designed according to ASCE 7-05. Journal of Structural Engineering, **137**(5), 589-599.

Farzampour, A. and Eatherton, M.R. (2018a). Investigating limit states for butterfly-shaped and straight shear links, Proc. of the 16th European Conference on Earthquake Engineering, 16ECEE, Thessaloniki, Greece.

Farzampour, A. and Eatherton, M.R. (2018b). Parametric study on butterfly-shaped shear links with various geometries, Proc. of the 11th National Conference on Earthquake Engineering, 11NCEE, Los Angeles, USA.

FEMAP695 (2009), "Quantification of Building Seismic Performance Factors", Washington, D.C.

FIP Industriale Company, Italy.

Gao, N., Jeon, J.-S., Hodgson, D.E. and DesRoches, R. (2016). An innovative seismic bracing system based on a superelastic shape memory alloy ring. Smart Materials and Structures, **25**(5), 055030-055030.

Hedayati Dezfuli, F. and Alam, M.S. (2015). Hysteresis model of shape memory alloy wire-based laminated rubber bearing under compression and unidirectional shear loadings. Smart Materials and Structures, **24**(6), 065022-065022.

Hedayati Dezfuli, F. and Alam, M.S. (2017). Smart lead rubber bearings equipped with ferrous shape memory alloy wires for seismically isolating highway bridges. Journal of Earthquake Engineering, **22**(6), 1042-1067.

Hu, J.W. (2008). *Seismic performance evaluations and analyses for composite moment frames with smart SMA PR-CFT connections.* Georgia Institute of Technology.

Hu, J.W. (2016). Seismic analysis and parametric study of SDOF lead-rubber bearing (LRB) isolation systems with recentering shape memory alloy (SMA) bending bars. Journal of Mechanical Science and Technology, **30**(7), 2987-2999.

Hu, J.W. and Leon, R.T. (2011). Analyses and evaluations for composite-moment frames with SMA PR-CFT connections. Nonlinear Dynamics, **65**(4), 433-455.

Kazemzadeh Azad, S. and Topkaya, C. (2017). A review of research on steel eccentrically braced frames. Journal of Constructional Steel Research, **128**, 53-73.

Leblouba, M., Altoubat, S., Ekhlasur Rahman, M. and Palani Selvaraj, B. (2015). Elliptical leaf spring shock and vibration mounts with enhanced damping and energy dissipation capabilities using lead spring. Shock and Vibration, **2015**, 12.

Mansouri, I., Ghodrati Amiri, G., Hu, J.W., Khoshkalam, M., Soori, S. and Shahbazi, S. (2017). Seismic fragility estimates of LRB base isolated frames using performance-based design. Shock and Vibration, **2017**, 1-20.

Mansouri, I., Mirzai, N.M. and Saffari, H. (2012). Seismic reliability of eccentrically braced frames, Proc. of the 11th International Conference on Computational Structures Technology, CST2012, Dubrovnik, Croatia.

Montuori, R., Nastri, E. and Piluso, V. (2014a). Rigid-plastic analysis and moment-shear interaction for hierarchy criteria of inverted y EB-Frames. Journal of Constructional Steel Research, **95**, 71-80.

Montuori, R., Nastri, E. and Piluso, V. (2014b). Theory of plastic mechanism control for the seismic design of braced frames equipped with friction dampers. Mechanics Research Communications, **58**, 112-123.

Montuori, R., Nastri, E. and Piluso, V. (2015). Seismic response of EB-frames with inverted Y-scheme: TPMC versus eurocode provisions. Earthquake and Structures, **8**(5), 1191-1214.

Montuori, R., Nastri, E. and Piluso, V. (2016a). Preliminary analysis on the influence of the link configuration on seismic performances of MRF-EBF dual systems designed by TPMC. Ingegneria Sismica, **33**(3), 52-64.

Montuori, R., Nastri, E. and Piluso, V. (2016b). Theory of Plastic Mechanism Control for MRF-EBF dual systems: Closed form solution. Engineering Structures, **118**, 287-306.

Montuori, R., Nastri, E. and Piluso, V. (2017). Influence of the bracing scheme on seismic performances of MRF-EBF dual systems. Journal of Constructional Steel Research, **132**, 179-190.

Moradi, S. and Alam, M.S. (2015). Feasibility study of utilizing superelastic shape memory alloy plates in steel beam–column connections for improved seismic performance. Journal of Intelligent Material Systems and Structures, **26**(4), 463-475.

Nastri, E. (2016). Eccentrically braced frames designed for the energy dissipation optimization, Proc. of the 7th European Congress on Computational Methods in Applied Sciences and Engineering, ECCOMAS 2016, Greece, 8476-8491.

Nastri, E., Montuori, R. and Piluso, V. (2015). Seismic design of MRF-EBF dual systems with vertical links: EC8 vs plastic design. Journal of Earthquake Engineering, **19**(3), 480-504.

OpenSees Open System for Earthquake Engineering Simulation, http://opensees.berkeley.edu/wiki/index.php/Main_Page.

Petrone, G., Ferrentino, T. and Alfano, G. (2017). Influence of PGA/PGV ratio on the seismic reliability of base-isolated systems with FPS. Ingegneria Sismica, **34**(3-4), 39-61.

Popov, P.E. and Ricles, J.M. (1994). Inelastic link element for EBF. Journal of Structural Engineering, **120**(2), 441-463.

Ricles, J.M., Sause, R., Peng, S.W. and Lu, L.W. (2002). Experimental evaluation of earthquake resistant posttensioned steel connections. Journal of Structural Engineering, **128**(7), 850-859.

Rofooei, F.R. and Yadegari Farzaneh, A. (2016). Numerical study of an innovative SMA based beam-column connection in reducing the seismic response of steel MRF structures. Scientia Iranica, **23**(5), 2033-2043.

Roh, J.-E., Hur, M.-W., Choi, H.-H. and Lee, S.-H. (2018). Development of a Multiaction Hybrid Damper for Passive Energy Dissipation. Shock and Vibration, **2018**, 16.

Seo, J., Kim, Y.C. and Hu, J.W. (2015). Pilot study for investigating the cyclic behavior of slit damper systems with recentering shape memory alloy (SMA) bending bars used for seismic restrainers. Applied Sciences (Switzerland), **5**(3), 187-208.

Silwal, B., Ozbulut, O.E. and Michael, R.J. (2016). Seismic collapse evaluation of steel moment resisting frames with superelastic viscous damper. Journal of Constructional Steel Research, **126**, 26-36.

Vamvatsikos, D. and Cornell, A.C. (2002). Incremental dynamic analysis. Earthquake Engineering and Structural Dynamics, **31**(3), 491-514.

Xu, X., Zhang, Y. and Luo, Y. (2016). Self-centering eccentrically braced frames using shape memory alloy bolts and post-tensioned tendons. Journal of Constructional Steel Research, **125**, 190-204.

Zareie, S., Mirzai, N.M., Alam, S. and Seethaler, R. (2017a). A dynamic analysis of a novel shape memory alloy-based bracing system, Proc. of the 6th International Conference on Engineering Mechanics and Materials, CSCE, Vancouver, Canada.

Zareie, S., Mirzai, N.M., Alam, S. and Seethaler, R. (2017b). A introduction and modeling of novel shape memory alloy-based bracing, Proc. of the 6th International Conference on Engineering Mechanics and Materials, CSCE, Vancouver, Canada.

Zeynali, K., Saeed Monir, H., Mirzai, N.M. and Hu, J.W. (2018). Experimental and numerical investigation of lead-rubber dampers in chevron concentrically braced frames. Archives of Civil and Mechanical Engineering, **18**(1), 162-178.

ingegneria sismica
International Journal of Earthquake Engineering
Anno XXXV – Num.4

ANALISI DELLE PRESTAZIONI SISMICHE DI CONTROVENTI ECCENTRICI CON LINK VERTICALI DOTATI DI UN NUOVO SISTEMA SMORZANTE AUTO-RICENTRANTE

Nadia M. Mirzai[1], *Reza Attarnejad*[2], *Jong Wan Hu*[3,4]

[1]School of Civil Engineering, College of Engineering, University of Tehran, P.O. Box 4563-11155, Tehran, Iran, E-mail: nmirzai@ut.ac.ir

[2]School of Civil Engineering, College of Engineering, University of Tehran, P.O. Box 4563-11155, Tehran, Iran, E-mail: attarnjd@ut.ac.ir

[3]Department of Civil and Environmental Engineering, Incheon National University, Incheon 22012, South Korea, E-mail: jongp24@inu.ac.kr

[4]Incheon Disaster Prevention Research Center, Incheon National University, Incheon 22012, South Korea

SUMMARY: *I sistemi sismoresistenti convenzionali possono essere soggetti a deformazioni e danni permanenti a seguito di forti eventi sismici che possono indurre a considerevoli costi di riparazione post-terremoto. Questo articolo presenta un modo semplice e veloce per ridurre la domanda di rotazione plastica dei link, la rotazione plastica residua, i costi e i tempi di riparazione. Esso si basa su un sistema per l'adeguamento sismico dei controventati eccentrici ad Y inversa (EBF) che è anche un sistema di ricentraggio che combina le leghe a memoria di forma ed i dissipatori gomma piombo (SMA-LRD). Controventi eccentrici a 4 e 9 piani sono stati progettati ed analizzati con e senza il sistema proposto mediante il software OpenSees. Più di 5000 analisi non lineari sono state sviluppate per valutare le performances sismiche di questi dissipatori ibridi usando 28 terremoti reali. I risultati delle analisi dinamiche incrementali (IDA) mostrano che implementando il nuovo sistema conduce a considerevoli riduzioni in termini di drift massimo, drift residuo e spostamenti residui..*

KEYWORDS: *Self-centering, SMA, LRD, EBF, Residual drift, OpenSees, IDA*

Corresponding author: Jong Wan Hu, Department of Civil Engineering, Incheon National University, Incheon 22012, South Korea, E-mail: jongp24@inu.ac.kr